BIOCHEMISTRY
including biophysical chemistry & molecular biology

ARTICLE

pubs.acs.org/biochemistry

A Quantitative Analysis of the Effect of Nucleotides and the M Domain on the Association Equilibrium of ClpB

Urko del Castillo,[†] Carlos Alfonso,[‡] Sergio P. Acebrón,[†,§] Ariadna Martos,[‡] Fernando Moro,[†] Germán Rivas,[*,‡] and Arturo Muga[*,†]

[†]Unidad de Biofísica (Consejo Superior de Investigaciones Científicas/Universidad del País Vasco-Euskal Herriko Unibertsitatea) and Departamento de Bioquímica y Biología Molecular, Universidad del País Vasco, Bilbao 48080, Spain

[‡]Centro de Investigaciones Biológicas (Consejo Superior de Investigaciones Científicas), Ramiro de Maeztu 9, Madrid 28040, Spain

S *Supporting Information*

ABSTRACT: ClpB is a hexameric molecular chaperone that, together with the DnaK system, has the ability to disaggregate stress-denatured proteins. The hexamer is a highly dynamic complex, able to reshuffle subunits. To further characterize the biological implications of the ClpB oligomerization state, the association equilibrium of the wild-type (wt) protein and of two deletion mutants, which lack part or the whole M domain, was quantitatively analyzed under different experimental conditions, using several biophysical [analytical ultracentrifugation, composition-gradient (CG) static light scattering, and circular dichroism] and biochemical (ATPase and chaperone activity) methods. We have found that (i) ClpB self-associates from monomers to form hexamers and higher-order oligomers that have been tentatively assigned to dodecamers, (ii) oligomer dissociation is not accompanied by modifications of the protein secondary structure, (iii) the M domain is engaged in intersubunit interactions that stabilize the protein hexamer, and (iv) the nucleotide-induced rearrangement of ClpB affects the protein oligomeric core, in addition to the proposed radial extension of the M domain. The difference in the stability of the ATP- and ADP-bound states [$\Delta\Delta G_{(ATP-ADP)} = -10$ kJ/mol] might explain how nucleotide exchange promotes the conformational change of the protein particle that drives its functional cycle.

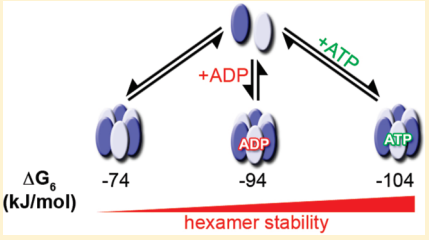

Many essential processes such as membrane fusion, organelle biogenesis, cell cycle regulation, and protein repair and degradation are mediated in all organisms by members of the AAA+ (ATPase associated with various cellular activities) superfamily.[1−3] Hsp100 proteins belong to this superfamily and are central components of the protein quality control system that degrade or disaggregate unfolded and aggregated proteins.[4−6] The bacterial ClpB and its homologue in yeast, Hsp104, are able to solubilize and reactivate protein aggregates that were previously viewed as dead-end products in the life of proteins.[7,8] This remarkable ability requires the cooperation of two chaperone systems, Hsp70 and Hsp100,[9−12] and is essential for the ability of cells to survive transient extreme stress conditions.[13,14]

As a member of the family of class I AAA+ proteins, ClpB contains an N-terminal domain, two nucleotide binding domains (NBDs) separated by a central domain, and a C-terminal region.[15] ClpB assembles into a hexameric ring that seems to be the functional unit of the chaperone. The N-terminal domain is assumed to play a role in substrate recognition but appears to be dispensable for its ability to disaggregate small aggregates *in vitro*.[16,17] The C-terminal region is involved in subunit oligomerization,[18] and both NBDs bind and hydrolyze ATP, the motor driving nucleotide-mediated protein disaggregation.[19] The M domain, which is specific for ClpB and its homologues, is inserted into NBD1 and forms a structure built by four helices that sticks out from the protomer like an arm in the X-ray structure of $ClpB_{Th}$.[20,21] M domains are strictly required for protein disaggregation[22−25] and exhibit nucleotide-dependent conformational changes during the ClpB ATPase cycle.[21] Although initially proposed to act as a molecular "crowbar", allowing ClpB to disrupt protein aggregates,[20] M domains appear now as regulatory devices that couple the initial Hsp70 chaperone activity with the threading activity of ClpB for efficient protein disaggregation.[26]

The oligomeric state of ClpB and Hsp104 has been extensively investigated. These studies have shown that their hexameric species are not very stable and exchange subunits in solution[27] on a time scale similar to that of steady-state ATP hydrolysis.[28] The association equilibrium can be modulated by ligand binding and salt or protein concentration.[22,23,29−32] Despite the fact that ClpB, like other AAA+ proteins, acts efficiently only in oligomeric assemblies, the quantitative characterization of this equilibrium has not been attempted before. We quantitatively investigate the self-association of ClpB under different experimental conditions (protein and salt concentrations and nucleotides) and model the experimental data using previously proposed[7,32] and new association schemes. Interestingly, those

Received: October 17, 2010
Revised: January 18, 2011
Published: February 10, 2011

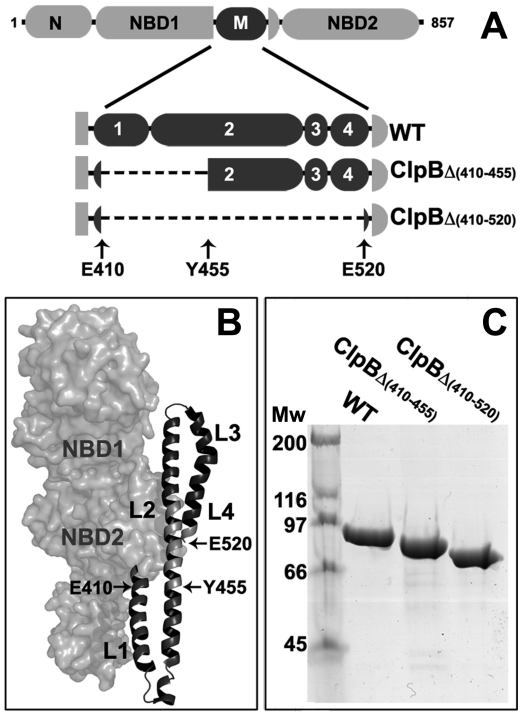

Figure 1. Domain organization of wt ClpB and the M domain deletion mutants characterized in this study. ClpB consists of an N-terminal domain, two nucleotide binding domains (NBD1 and NBD2), and an M domain inserted into NBD1. (A) Deletion mutants $ClpB_{\Delta(410-455)}$ and $ClpB_{\Delta(410-520)}$ in which the M domain was partially or totally deleted. (B) Structure of $ClpB_{Th}$ (Protein Data Bank entry 1QVR) displayed with the M domain represented as a ribbon and the deletion points highlighted. This structure was drawn with MacPyMol. (C) Sodium dodecyl sulfate−polyacrylamide gel electrophoresis analysis of purified wt ClpB, $ClpB_{\Delta(410-455)}$, and $ClpB_{\Delta(410-520)}$.

that better fit the data include higher-order oligomers that we have tentatively assigned to dodecamers, because it was the simplest larger oligomer possible, that were not described previously. We also show that the ATP-bound ClpB hexamer is 10 kJ/mol more stable than the ADP state, suggesting that nucleotide exchange could facilitate oligomer rearrangement during its functional cycle. The comparison of the free energy of subunit association of wild-type (wt) ClpB and two M domain deletion mutants that lack motif 1 or the entire domain (Figure 1) also demonstrates that the M domain, and in particular motif 1 of this domain, stabilizes the protein hexamer.

MATERIALS AND METHODS

Protein Expression and Purification. wt ClpB and ClpB deletion mutants were expressed in *Escherichia coli* strain BB4561 and purified as previously reported.[33] To clone $ClpB_{\Delta(410-455)}$ and $ClpB_{\Delta(410-520)}$ deletion mutants, a 1.2 kb fragment was amplified by polymerase chain reaction using the primers 5′-CCCGAATTCATTAAAGAGG-3′ and 5′-CCCGAGCTCTTC-GAATCAATCTGCATACGA-3′ and the pUHE21-ClpB expression plasmid as the template. A second fragment of 1 kb was amplified by the primers 5′-CCCCTTCGAAACCATCCGAGT-TAGAAGAAGAG-3′ [for $ClpB_{\Delta(410-455)}$] or 5′-CCCCTTCGA-AACCAGGCAAAACTATGCGTCTG-3′ [for $ClpB_{\Delta(410-520)}$] and 5′-CCCGAATTCCGGACGGAAG-3′. Then the 1.2 kb EcoRI/BstBI and 1 kb BstBI/EcoRI fragments were inserted into the EcoRI-digested pUHE21-ClpB expression vector. DnaK, DnaJ, and GrpE were expressed in BL21(DH3) cells and purified as described previously.[34−36] Protein concentrations were determined by the Bradford method (Bio-Rad) and expressed in moles of ClpB monomer. The molar masses of monomeric wt ClpB, $ClpB_{\Delta(410-455)}$, and $ClpB_{\Delta(410-520)}$ were 95585, 90096, and 82799 Da, respectively.

Size-Exclusion Chromatography (SEC). Wild-type ClpB or ClpB mutants (50 μM monomer) were loaded on a Superose 6 PC 3.2/30 column (GE Healthcare) equilibrated in 50 mM Hepes (pH 7.5), 5 mM $MgCl_2$, and the desired KCl concentration (20−500 mM).

Circular Dichroism. Far-UV CD spectra were recorded on a Jasco (Tokyo, Japan) J-180 spectropolarimeter equipped with a thermoelectric cell holder using a 1 mm path length cuvette. Samples contained 10 μM protein monomer in 50 mM Hepes-KOH (pH 7.5), 5 mM $MgCl_2$, and the desired KCl concentration. Five spectra were recorded between 260 and 190 nm at 25 °C and averaged. In urea-induced unfolding studies, the protein (10 μM) was incubated overnight at 4 °C in buffer containing 50 mM Tris (pH 7.5), 5 mM $MgCl_2$, 20 or 500 mM KCl, and increasing urea concentrations, and the ellipticity at 222 nm was measured at 25 °C after equilibration for 1 h at room temperature. To obtain the unfolding free energy of monomeric ClpB, a two-state equilibrium between native and unfolded protein was assumed under experimental conditions in which ClpB hexamer completely dissociates into monomers. The fraction of native protein was obtained from the expression $f_N = ([Q]_i - [Q]_U)/([Q]_N - [Q]_U)$, where $[Q]_i$ is the measured ellipticity at 222 nm for each urea concentration and $[Q]_N$ and $[Q]_U$ are the ellipticity values of the native and unfolded states, respectively. The apparent unfolding free energy at each point was obtained from the equation $\Delta G_{app} = -RT \ln[(1 - f_N)/f_N]$ and plotted versus urea concentration. The free energy of unfolding in the absence of urea was estimated by the linear extrapolation method.[37]

ATPase Activity. Steady-state ATPase activity measurements were performed in 50 mM Tris-HCl (pH 7.5) buffer containing 5 mM $MgCl_2$ and the desired KCl concentration (20−700 mM) at 25 °C, as described previously,[34] in the presence of an ATP-regenerating system.[38] Protein and ATP concentrations were 2 or 10 μM and 1 mM, respectively. Substrate-induced stimulation of the ATPase activity was assessed in the presence of 10 or 25 μM α-casein at a ClpB concentration of 2 or 10 μM, respectively (Sigma). Reactions were followed by measuring the absorbance decay at 340 nm in a Cary spectrophotometer (Varian).

Protein Aggregate Reactivation. Luciferase (2.5 μM, Roche) was denatured for 45 min at 25 °C, in 7 M urea, 30 mM Hepes (pH 7.4), 60 mM KCl, 10 mM $MgCl_2$, and 10 mM DTT. Denatured protein was diluted to 25 nM in 30 mM Hepes (pH 7.4), 20 mM KCl, 10 mM $MgCl_2$, and 2 mM DTT, containing an ATP-regenerating system (8 or 20 mM phosphoenolpyruvate in samples containing 1.5 or 10 μM ClpB, respectively, and 20 ng/mL pyruvate kinase), and incubated for 10 min. Then, chaperones (1.5 or 10 μM ClpB, 1 μM DnaK, 0.1 μM DnaJ, and 0.5 μM GrpE) were added, and the KCl concentration was adjusted. Reactivation was initiated by adition of 2 mM ATP. Luciferase activity was measured after reactivation for 120 min at 25 °C using the luciferase assay system (Promega E1500) in a Sinergy HT (Biotek) luminometer.

The salt dependence of the chaperone activity of K/J/E alone was assayed using luciferase (2.5 μM) denatured for 45 min at

25 °C in 6 M Gdn-HCl, 100 mM Tris (pH 7.7), and 10 mM dithiothreitol. Refolding was achieved via dilution of luciferase to 25 nM in 50 mM Tris (pH 7.7), 15 mM $MgCl_2$, and 5.5 mM dithiothreitol. The refolding buffer also contained an ATP-regenerating system (8 mM phosphoenolpyruvate and 20 ng/mL pyruvate kinase) and the desired KCl concentration. Finally, the chaperones (1 μM DnaK, 1 μM DnaJ, and 1.2 μM GrpE) were added, and the reactivation was initiated by addition of 5 mM ATP. Luciferase activity was measured after reactivation for 90 min as described above.

MDH (4 μM monomer, Sigma) was denatured and aggregated via incubation of the protein for 30 min at 47 °C in 50 mM Tris-HCl, 100 mM KCl, 5 mM $MgCl_2$, and 2 mM DTT (pH 7.5). The sample was diluted (final concentration of 1 μM) in the presence of 1.5 or 10 μM ClpB, 1 μM DnaK, 0.3 μM DnaJ, and 0.2 μM GrpE in buffer containing different KCl concentrations. Reactivation was started via addition of 2 mM ATP to the sample containing an ATP regenerating system (8 or 20 mM phosphoenolpyruvate in samples containing 1.5 or 10 μM ClpB, respectively, and 20 ng/mL pyruvate kinase) at 30 °C. MDH activity was recorded after reactivation for 3 h as previously described.[39]

Analytical Ultracentrifugation. Sedimentation analysis of wt ClpB and deletion mutants was performed at several protein concentrations (1−50 μM monomer). All samples were in 50 mM Tris-HCl (pH 7.5) and 5 mM $MgCl_2$ buffer containing different KCl concentrations (20−500 mM). Sedimentation velocity experiments were conducted at 40000 rpm and 18 °C in an XL-A analytical ultracentrifuge (Beckman-Coulter Inc.) with an UV−vis optics detection system, using an An50Ti rotor and 12 mm double-sector centerpieces. Sedimentation profiles were registered every 5−7 min at 285 nm. The sedimentation coefficient distributions were calculated by least-squares boundary modeling of sedimentation velocity data using the $c(s)$ method,[40,41] as implemented in SEDFIT. These s values were corrected to standard conditions (water, 20 °C, and infinite dilution)[42] using SEDNTERP,[43] yielding the corresponding standard s values ($s_{20,w}$). The effect of nucleotides was analyzed in samples that contained, besides the reagents mentioned above, 1 mM ADP or ATP. The last samples also contained an ATP-regenerating system (10 mM acetyl phosphate and 1 unit/mL acetyl kinase) that kept the nucleotide concentration cons tant during the time required to run a sedimentation velocity experiment (3 h).

Sedimentation equilibrium experiments were performed to determine the size and self-association properties of ClpB as a function of salt and protein concentration at several speeds (4000, 6000, and 9000 rpm) and wavelengths (from 230 to 300 nm), using short columns (85 μL) and the same experimental protocol described above. After the equilibrium scans, a high-speed centrifugation run (40000 rpm) was conducted to estimate the corresponding baseline offsets. The measured equilibrium concentration (signal) gradients of ClpB were fit by the equation that characterizes the equilibrium gradient of an ideally sedimenting solute,[44] yielding the corresponding whole-cell signal average molecular weights (M_W), using 0.737 mL/g as the partial specific volume of ClpB (calculated from the amino acid composition using SEDNTERP).[43] The analysis of the dependence of M_W on ClpB concentration was performed as described in the modeling self-association section.

Composition-Gradient Static Light Scattering (CG-SLS). The CG-SLS procedure recently developed by Minton and coworkers[45] was essentially followed. In brief, a programmable three-injector syringe pump (CALYPSO, Wyatt Technology, Santa Barbara, CA) was used to introduce a solution with a defined protein composition (that changes in consecutive injections) into parallel flow cells to concomitantly measure Rayleigh light scattering at multiple angles (using a DAWN-EOS multiangle laser light scattering detector, Wyatt Technology) and solute concentrations (using an Optilab rEX refractive index detector, Wyatt Technology). The experiment yields several thousand values of the Rayleigh ratio as a function of protein concentration and scattering angle. Typically, 10 injections of different protein concentrations and 2 mM nucleotide were mixed, and the light scattering and refraction index of the resulting mixture were measured for 2 min. These experimental conditions ensured that less than 3% of the initially added ATP was hydrolyzed during the experiment. All the composition and angular dependence data were then analyzed in the context of association models, as described below, yielding the molecular masses, complex stoichiometry, and equilibrium constants of ClpB under different experimental conditions. Samples contained increasing protein concentrations (0−5 μM) in 50 mM Tris-HCl (pH 7.5), 5 mM $MgCl_2$, and 150 mM KCl. The effect of salt on the oligomerization state of wt ClpB was also analyzed using 10 μM monomer protein solutions in 50 mM Tris-HCl and 5 mM $MgCl_2$ (pH 7.5).

Models for ClpB Self-Association. The scaled Rayleigh ratio of a dilute solution containing a single scattering component (in our case, ClpB) is given by[46]

$$R/K_{opt} = \sum_i M_i w_i = M_W w_{tot} \quad (1)$$

where M_i and w_i denote the molecular weight and weight/volume ratio of each oligomeric state of ClpB, respectively, w_{tot} is the total weight/volume ratio, and M_W is the weight-average molecular weight, given by

$$M_W = \sum_i w_i M_i / \sum_i w_i \quad (2)$$

It follows from eq 1 that any equilibrium model used to fit the dependence of R/K_{opt} on w_{tot} may also be used to calculate the dependence of M_W on w_{tot}, the form in which the sedimentation equilibrium results are presented in this work. Therefore, the same association schemes described below have been used to model the composition dependence data of both light scattering and sedimentation equilibrium experiments.

The uncertainty of the value of various parameters was estimated via least-squares modeling using a variation of the sum-of-squares profile method described by Saroff.[47] A Fisher F test was applied to determine the probability P_{reject} with which a particular constrained fit, as quantified by the variance of estimate, may be regarded as statistically significantly inferior to the best fit (i.e., rejected). The probability of acceptance P_{accept} was defined as $1 - P_{reject}$. The uncertainty of the best-fit parameter P^* reported in Results and Discussion represents the minimal and maximal values for which P_{accept} exceeds 0.05 (95% confidence limits, or two standard errors of the estimate).

Monomer−Dimer−Hexamer−Dodecamer Model (1−2−6−12). Consider ClpB existing as an equilibrium mixture of monomers, dimers, hexamers, and dodecamers with equilibrium constants given by

$$K_2 = w_2/{w_1}^2 \quad (3)$$

$$K_6 = w_6/{w_1}^6 \quad (4)$$

$$K_{12} = w_{12}/{w_1}^{12} \quad (5)$$

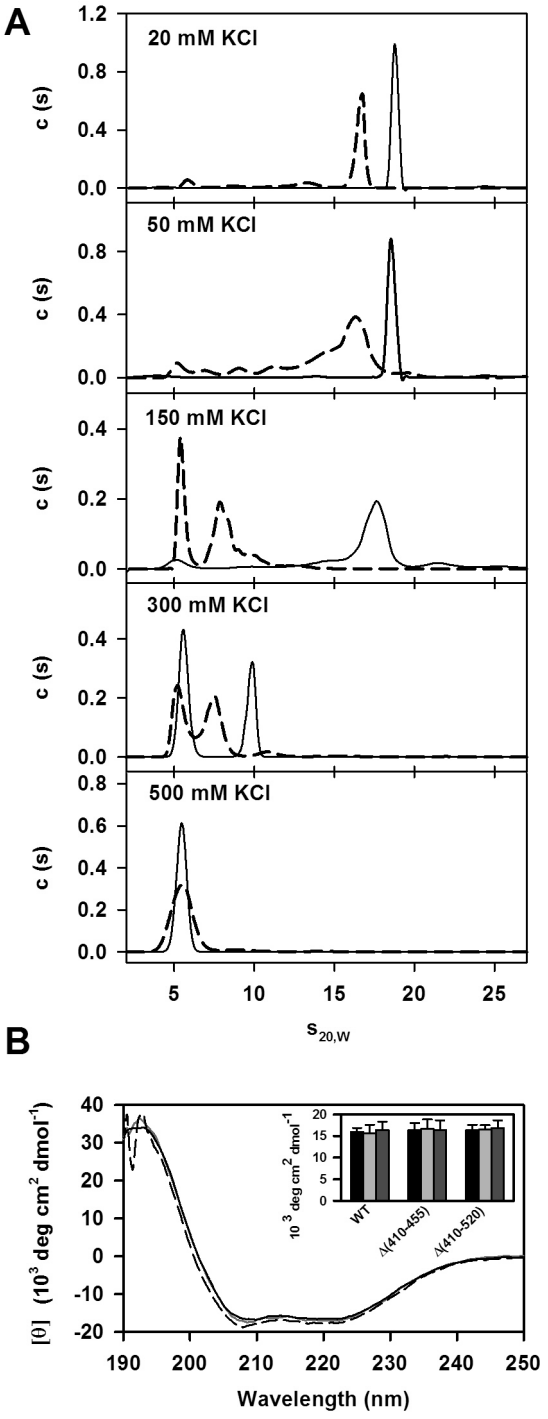

Figure 2. Effect of KCl on wt ClpB and $ClpB_{\Delta(410-455)}$ oligomerization state: sedimentation velocity and CD analysis. (A) Sedimentation coefficient distribution of 10 μM monomer wt ClpB (—) and $ClpB_{\Delta(410-455)}$ (– – –) at increasing salt concentrations. (B) Far-UV circular dichroism spectra of 10 μM monomer wt ClpB in 50 mM Hepes (pH 7.5), 5 mM $MgCl_2$, and 20 (black solid line), 150 (gray solid line), or 500 mM KCl (dashed line). The inset shows molar ellipticity values at 222 nm for wt ClpB and deletion mutants in buffer containing 20 (black bars), 150 (light gray bars), or 500 mM KCl (dark gray bars).

where w_1, w_2, w_6, and w_{12} are the weight concentrations of monomers, dimers, hexamers, and dodecamers, respectively. The total concentration is given by

$$w_{tot} = w_1 + w_2 + w_6 + w_{12} \quad (6)$$

Given the values of w_{tot}, M_1, and the three association constants, eqs 3−6 were solved numerically for the equilibrium value of w_1, and then eqs 3−5 were used to calculate the equilibrium values of the different oligomeric species. Then eq 2 was used to calculate M_W and eq 1 to calculate R/K_{opt}. All the calculations were performed using MATLAB scritps kindly provided by A. Minton (National Institutes of Health, Bethesda, MD).

Monomer−Trimer−Hexamer−Dodecamer Model (1−3−6−12). This association scheme is analogous to the previous one with dimers being substituted with trimers.

Monomer−Hexamer−Dodecamer Model (1−6−12). This model is defined by the equilibrium constants.

$$K_6 = w_6/{w_1}^6 \quad (7)$$

$$K_{12} = w_{12}/{w_1}^{12} \quad (8)$$

where w_1, w_6, and w_{12} are the weight concentrations of monomers, hexamers, and dodecamers, respectively.

The total concentration is given by

$$w_{tot} = w_1 + w_6 + w_{12} \quad (9)$$

As mentioned above, eqs 7−9 were used to calculate the equilibrium values of w_1, w_6, and w_{12}. Then eqs 1 and 2 were used to calculate R/K_{opt} and M_W, respectively.

Monomer−Dimer−Heptamer Model (1−2−7). This is the model used in ref 31 to account for their sedimentation equilibrium results. The model is defined by two equilibrium constants.

$$K_2 = w_2/{w_1}^2 \quad (10)$$

$$K_7 = w_7/{w_1}^7 \quad (11)$$

In this case, the total protein concentration is given by

$$w_{tot} = w_1 + w_2 + w_7 \quad (12)$$

In a manner similar to that in the monomer−hexamer−dodecamer model, eqs 10−12 were used to calculate the equilibrium values of w_1, w_2, and w_7. Then eqs 1 and 2 were used to calculate R/K_{opt} and M_W, respectively.

RESULTS AND DISCUSSION

The M Domain Stabilizes ClpB Oligomers. The effect of the M domain on the previously reported dependence of the protein oligomerization state on salt concentration was first analyzed by gel filtration chromatography (Figure S1 of the Supporting Information). Increasing KCl concentrations induced oligomer dissociation, as seen by the increase in the elution volume values, in agreement with previous observations.[10,48] A similar effect was observed for both M domain deletion mutants at lower salt concentrations. Proteins were also characterized by analytical ultracentrifugation under the same experimental conditions. The sedimentation coefficient distributions of wt ClpB (10 μM monomer) as a function of salt concentration are shown in Figure 2A. Below 150 mM KCl, ClpB sedimented as a major single species with an $s_{20,w}$ value of 18.5 ± 0.5 S. Additionally, less abundant (<10%) species with $s_{20,w}$ values of approximately 23 S were also found (Figure S2 of the Supporting Information). The sedimentation equilibrium gradients of these samples were compatible with a major ideally sedimenting solute with an average molecular weight of 628000 ± 30000 (Figure S3 of

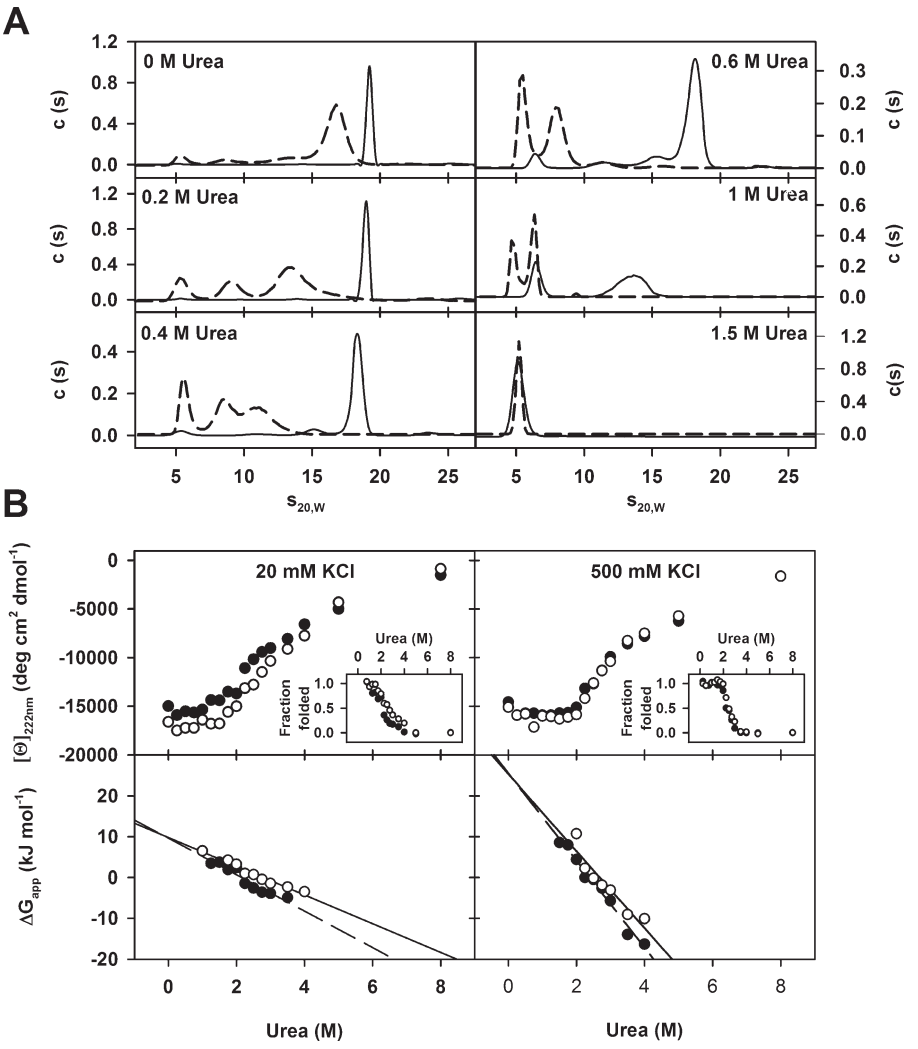

Figure 3. Stability of hexameric and monomeric species of wt ClpB and $ClpB_{\Delta(410-455)}$. (A) Sedimentation coefficient distribution of 10 μM wt ClpB (—) and $ClpB_{\Delta(410-455)}$ (– – –) at increasing urea concentrations. (B) Urea denaturation profiles (top) of wt ClpB (○) and $ClpB_{\Delta(410-455)}$ (●) followed by the change in molar ellipticity at 222 nm in buffer containing 20 (left) or 500 mM KCl (right). The insets show the fraction of folded wt ClpB (○) and $ClpB_{\Delta(410-455)}$ (●) as a function of urea concentration. The apparent free energy of unfolding in the presence of urea versus denaturant concentrations is shown in the bottom panels. Solid and dashed lines represent the linear regression of the data for ClpB and $ClpB_{\Delta(410-455)}$, respectively.

the Supporting Information). This value was higher than that obtained from the sequence of the ClpB hexamer (573510), suggesting the possible presence of higher-order oligomers. At 150 mM KCl, the sedimentation coefficient distribution was broader and quantitatively described by significant contributions of sedimenting species with $s_{20,w}$ values of 5.2, 14.3, and 17.7 S. This polydispersity is not unambiguous proof of the existence of these intermediate species as very complex boundary profiles may be obtained depending upon the kinetics of ClpB association and dissociation, which is currently not well understood. At higher salt concentrations, the sedimentation coefficient distributions exhibited a greater abundance of more slowly sedimenting species because of oligomer dissociation, as expected from the gel filtration experiments. The sedimentation velocity profile of ClpB at 300 mM KCl was described well by two main species with $s_{20,w}$ values of 5.5 and 9.4 S, while at 500 mM KCl, the protein sedimented as a single species with an $s_{20,w}$ value of 5.5 ± 0.5 S and an average molecular weight of 100000 ± 10000 (sedimentation equilibrium) or 124000 ± 8000 (static light scattering) (Figure S3 of the Supporting Information). The dependence of the excess light scattering of ClpB (10 μM) on KCl concentration confirmed that dissociation of the 18.5 S oligomer occurred between 150 and 400 mM KCl (Figure S4 of the Supporting Information). To investigate the reversibility of the association equilibrium, parallel experiments in which the salt concentration was either increased (from 20 to 500 mM KCl) or reduced (from 500 to 20 mM KCl) were conducted. The results were the same within experimental error (not shown).

Dissociation of M domain deletion mutants occurred at KCl concentrations lower than that for the wt protein, as demonstrated by sedimentation velocity measurements (Figure 2A). The experimental data of mutant $ClpB_{\Delta(410-455)}$ at 50 mM KCl were quantitatively described assuming significant contributions of sedimenting species with $s_{20,w}$ values from 5.3 to 16.6 S, indicating oligomer dissociation under conditions that supported wt ClpB oligomers. At 150 mM KCl, there was no evidence of 16.6 S oligomeric species, in contrast to what was seen for wt ClpB. A similar dissociation behavior was found for $ClpB_{\Delta(410-520)}$

(data not shown). It has been reported that elimination of selected regions of the M domain resulted in oligomerization defects,[23] and that truncation of the entire domain rendered protein hexamers.[22] This apparent discrepancy might be explained if the presence of mixtures of full-length ClpB and the naturally occurring N-terminally truncated form of the protein would compromise hexamer formation by the M domain deletion mutants.[23] Our data demonstrate that ClpB lacking the M domain retains the ability to form hexamers, although they are less stable than the wt oligomers.

Dissociation of oligomeric proteins can proceed through structured intermediates or alternatively can be coupled to monomer (partial) unfolding. To test which of these alternatives was more plausible, the far-UV CD spectrum of wt ClpB was measured at increasing KCl concentrations (Figure 2B). The spectrum showed the characteristic shape of a highly helical structure, a negative double band with minima at 208 and 222 nm, that is maintained within the KCl concentration range assayed (20−500 mM). The same salt dependence was observed for both deletion mutants (Figure 2B, inset). Deletion of the putative helical M domain did not induce the expected decrease in protein helicity, suggesting that specific regions of this domain might adopt conformations other than helical, as it has been proposed for the flexible helix 3 of motif 2.[26] Data presented so far indicate that increasing KCl concentrations induced dissociation of ClpB into structured monomers and that the M domain was involved in oligomer stabilization.

Urea was also used to induce ClpB oligomer dissociation and unfolding. First, sedimentation velocity experiments were conducted at 20 mM KCl, conditions under which wt ClpB is mainly present as 19.0 S oligomeric species in the absence of urea. Urea concentrations of <0.5 M had a weak effect on the sedimentation coefficient distribution of ClpB (Figure 3A). Oligomers with lower $s_{20,w}$ values were clearly observed above 0.5 M urea, which sedimented as monomeric 5.3 S species above 1.5 M denaturant (Figure 3A). Partial (Figure 3A) or complete (not shown) truncation of the M domain resulted in oligomer dissociation at lower urea concentrations, suggesting, as proposed above, that this domain stabilizes protein oligomers. To define the folding status of urea-induced protein (wt and mutant) monomers, the ellipticity at 222 nm of both polypeptides was measured at increasing urea concentrations (Figure 3B). The values characteristic of native wt ClpB and $ClpB_{\Delta(410-455)}$, i.e., those obtained in the absence of urea, were maintained up to 1.5 M urea, at which point the proteins are fully monomeric. Increasing urea concentrations induced a decrease in the ellipticity value that approached zero at 8 M, indicating complete unfolding of the protein monomer (Figure S5 of the Supporting Information). Therefore, urea-induced unfolding of wt ClpB and $ClpB_{\Delta(410-455)}$ proceeded through two main steps, namely, dissociation of the oligomer into structured monomers and monomer unfolding. The effect of the M domain on the stability of the monomer was examined under two experimental conditions: (i) low salt concentration (20 mM KCl), starting from 19.0 S oligomers and following the ellipticity change related to protein monomer unfolding above 1.5 M urea, and (ii) high salt concentration (500 mM KCl), to induce protein monomerization in the absence of urea. Analysis of the data (Figure 3B) indicated that the unfolding Gibbs free energies of monomeric wt ClpB and $ClpB_{\Delta(410-455)}$ were similar, although their values were considerably lower at 20 mM KCl [9.8 and 9.6 kJ/mol for wt ClpB and $ClpB_{\Delta(410-455)}$, respectively] than at 500 mM KCl (25.3 and 25.5 kJ/mol, respectively).

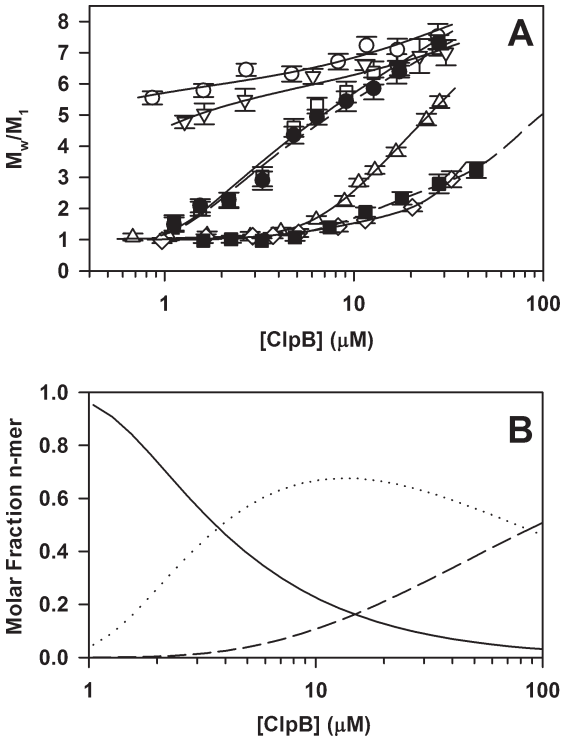

Figure 4. Effect of KCl on wt ClpB and $ClpB_{\Delta(410-455)}$ oligomerization state: sedimentation equilibrium analysis. (A) Dependence of the state of association (M_W/M_1) of wt ClpB and $ClpB_{\Delta(410-455)}$ on salt and protein concentration. Sedimentation equilibrium data are shown for wt ClpB at 50 (○), 100 (▽), 150 (□), 300 (△), and 500 mM KCl (◇). Sedimentation equilibrium data are shown for $ClpB_{\Delta(410-455)}$ at 50 (●) and 150 mM KCl (■). Solid (wt ClpB) and dashed [$ClpB_{\Delta(410-455)}$] lines were calculated using model 8 with best-fit parameter values given in Table 1. (B) Fractional distribution of monomer (—), hexamer (···), and dodecamer (− − −) species obtained from the best fit of the data corresponding to wt ClpB at 150 mM KCl shown in panel A.

These results pointed out that the M domain stabilized the ClpB oligomer and proved the existence of a structured monomer that could facilitate dissociation and association of the protein during its functional cycle, because it would not involve gross but rather local conformational changes of the structured monomer. Functionally, dissociation and reassembly of oligomeric ClpB have been related to the ability of the protein to avoid both blocking by very stable protein aggregates and unfolding of folded domains within the protein aggregate.[49] The location of the M domain within the structure of Hsp100 proteins remains controversial.[20,50] There are two alternative structures that, among other features, differ in the location of the M domain. The first cryoEM study of $ClpB_{Th}$[20] and cross-linking experiments suggested that motif 2 would be positioned between the NBD1 domains of neighboring subunits and could facilitate cooperative interactions in the NBD1 ring, while motif 1 would point away from the hexamer in the AMPPNP- and ATP-bound states.[21] A recent cryoEM study of Hsp104 has postulated an alternative structure in which the M domain would be intercalated between the NBDs,[51] instead of being projected outward from NBD1. In this model, the M domain would interact with NBD1 of the same subunit and contact NBD2 of the adjacent subunit through the L1−L2 (motif 1) end. Although the mobile and highly flexible M domain can adopt different conformations in solution, the latter location within the ClpB hexamer

Table 1. Models Used To Fit the Sedimentation Equilibrium Data of Apo ClpB at 150 mM KCl, in Order of Increasing Complexity[a]

model	association scheme	best-fit χ^2	P (best-fit χ^2)
1	1−6	108.46	0.00
2	1−7	25.03	0.00
3	1−2−6	108.46	0.00
4	1−3−6	108.46	0.00
5	1−2−7	25.02	0.00
6	1−3−7	25.04	0.00
7	1−7−14	25.04	0.00
8	1−6−12	12.08	0.19
9	1−2−6−12	11.99	0.20
10	1−3−6−12	11.99	0.20

[a] The precision of the data allows us to rule out models 1−7 with 95% confidence (see Materials and Methods). The best-fit values of the association constants, expressed in molar concentration units ($K'_n = K_n M_1^{n-1}/n$), of models 8−10, with 95% confidence limits are as follows: for model 8, $\log K'_6 = 13.0 \pm 1.0$ and $\log K'_{12} = 22.0 \pm 2.0$; for model 9, $\log K'_2 = 0.5 \pm 0.2$, $\log K'_6 = 13.0 \pm 1.0$, and $\log K'_{12} = 21.9 \pm 1.4$; and for model 10, $\log K'_3 = 3.8 \pm 1.6$, $\log K'_6 = 12.9 \pm 1.1$, and $\log K'_{12} = 22.0 \pm 1.4$.

would engage motif 1, through its interaction with neighboring subunits, in the stabilization of the hexameric protein, as we observe here.

ClpB Monomers Associate To Form Hexamers and Higher-Order Oligomers. The quantitative analysis of ClpB self-association required a detailed study of the oligomerization reaction by means of sedimentation equilibrium measurements at different KCl and protein concentrations. The dependence of the state of association (M_W/M_1) of ClpB on protein and salt concentration (Figure 4A) indicated dissociation of large oligomers at low protein concentrations and ionic conditions that favored oligomer formation (50 mM KCl), and formation of intermediate oligomerization states at high protein concentrations and conditions that promoted dissociation of the oligomer into monomers (500 mM KCl). From these results, we can conclude that the hydrodynamic (sedimentation velocity) and thermodynamic (sedimentation equilibrium) data obtained for ClpB as a function of salt concentration are semiquantitatively in accord. The concentration of the ClpB monomer in *E. coli* has been estimated to be around 9 and 20 μM at 30 and 42 °C, respectively,[52] and interestingly, this is the protein concentration range in which the oligomerization equilibrium of the chaperone is most sensitive to changes in salt concentration. Although *in vivo* the dissociation−association reaction might be modulated by other factors, such as specific physiological ligands (see below) and the crowded cellular environment, it is important to note that the potassium concentration within *E. coli* cytoplasm can drastically increase in response to different stress conditions.[53]

Various models were used to fit data obtained at 150 mM KCl. These conditions were found to be appropriate for a quantitative analysis because both oligomeric and dissociated species were significantly populated at high and low protein concentrations, respectively. A model was considered to be consistent with the data (i.e., not excluded by the data) if the probability of the best-fit value of χ^2 for this particular model was less than that obtained from a random distribution [i.e., if this probability exceeds 0.05; 95% confidence limits or two standard errors of the estimate (see Materials and Methods for details)]. The results of this analysis showed that only models 8−10 satisfied the χ^2 criterion (Table 1). The assumption that hexamers (models 1, 3, and 4) or heptamers (models 2, 5, and 6) were the upper oligomeric species did not pass the statistical criterion. The parameters obtained with model 8 (Table 1), the simplest one that quantitatively accounted for the experimental data, were used to calculate the gradients shown in Figure 4A. Accordingly, ClpB exists in solution as an equilibrium mixture of monomers, hexamers, and higher-order species that we have tentatively assigned to dodecamers, because it was the simplest larger oligomer possible, with equilibrium constants K_6 and K_{12}. It should be noted that very similar theoretical curves were obtained with models 9 and 10, which introduce the presence of intermediate species (dimers and trimers) into the association scheme. Although the sedimentation velocity profiles at this salt concentration may suggest the presence of such intermediates (Figure 2), they did not unambiguously prove their existence as complex sedimentation boundaries of monomer−oligomer binary mixtures can arise from differences in the association kinetics (see, for example, Figure 2b of ref 54), in our case linked to salt effects. The mass fractional distribution of each species at 150 mM KCl, calculated from the best-fit parameter values of model 8, is depicted in Figure 4B as a function of protein concentration.

Two equilibrium association models have been proposed that differ in the hexameric or heptameric nature of the highest-order oligomer. The existence of heptameric ClpB seems contradictory; while it was postulated to exist in both apo and nucleotide-bound ClpB,[29] a more recent study suggested that it was detected only at low ionic strengths in the absence of nucleotide.[31] We propose the 1−6−12 association model, because it is the simplest one that quantitatively fits the sedimentation equilibrium and GC-SLS data (see below). If, as discussed above, oligomerization intermediates exist, their association constants would be sufficiently similar so that their fractional abundance would overlap with that of the hexamers, making their discrimination impossible.[55] The equilibrium data cannot be quantitatively described without taking into account a significant contribution of a higher-order species, the dodecamer being the simplest one. A minor protein fraction (~10% of the loading concentration) that sedimented faster than ClpB hexamers was also detected by sedimentation velocity. However, because its molecular weight did not reach saturation at the highest ClpB concentration used, data did not exclude formation of oligomeric structures other than dodecamers. Experimental limitations precluded the discrimination between different models of higher-order association, as it was not possible to further increase protein concentration. The existence of these higher-order species was not due to protein aging during the experiment because the same behavior was found in CG-SLS experiments (see below), which are much faster as the whole experiment takes less than 1 h to be completed.

The sedimentation equilibrium data of $ClpB_{\Delta(410-455)}$ as a function of protein concentration, together with the gradients estimated with the best-fit parameter values obtained with model 8, are shown in Figure 4A at 50 and 150 mM KCl. The oligomeric species dissociated at protein and salt concentrations higher and lower than those of the wt protein, respectively, demonstrating that partial [or complete (not shown)] deletion of the M domain diminished the stability of ClpB oligomers. The association behavior of the ClpB mutant at 150 mM KCl was similar to that of wt ClpB at 300−500 mM KCl (Table 2). Therefore, the sedimentation equilibrium data are in excellent agreement with

Table 2. Dependence of ClpB Self-Association on KCl Concentration[a]

protein	[KCl] (mM)	log K'_6[b]	log K'_{12}[b]	ΔG°_6[c] (kJ/mol)	ΔG°_{12}[c] (kJ/mol)
wt	50	20.9 ± 2.0	37.7 ± 3.5	−121	−219
wt	100	17.1 ± 2.5	30.3 ± 6.0	−99	−176
wt	150	13.0 ± 1.0	22.0 ± 2.0	−75	−128
wt	300	10.0 ± 4.5	15.3 ± 5.0	−58	−89
wt	500	7.3 ± 2.0	12.8 ± 3.5	−42	−74
$ClpB_{\Delta(410-455)}$	50	12.6 ± 1.0	19.8 ± 4.0	−73	−115
$ClpB_{\Delta(410-455)}$	150	8.9 ± 2.0	nd	−52	nd

[a] Model 8 was used to calculate the self-association parameters. [b] Association constants are expressed in molar units. [c] The standard-state free energy change was calculated from the relation $\Delta G^\circ_n = -2.3RT \log K_n$.

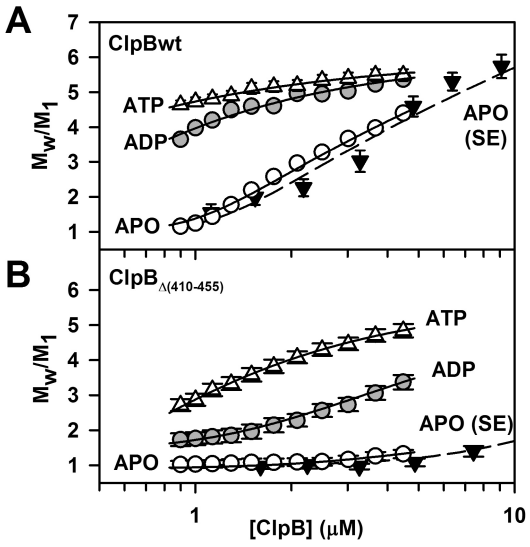

Figure 5. Effect of nucleotides on the association of wt ClpB and $ClpB_{\Delta(410-455)}$. M_W distribution normalized to the monomeric ClpB or $ClpB_{\Delta(410-455)}$ molecular weight (95585 or 90096, respectively) as a function of protein concentration. Experimental data corresponding to wt ClpB (A) or $ClpB_{\Delta(410-455)}$ (B) in the absence of nucleotide (○) and presence of ADP (gray circles) or ATP (△). For the sake of comparison, the sedimentation equilibrium results for the apoproteins are also shown (▼). Solid lines represent the M_W distribution as obtained from the best-fit parameter values listed in Table 3.

the sedimentation velocity results previously shown. The association free energy of the wt ClpB hexamer was 48 and 23 kJ/mol higher than that of $ClpB_{\Delta(410-455)}$ at 50 and 150 mM KCl, respectively, indicating that motif 1 of the M domain is involved in intersubunit interactions that modulate oligomer stability. A previous study using ClpB variants with single Trp residues in each protein structural domain suggested that NBD2 and to a lesser extent the M domain may undergo structural rearrangements during formation of the ClpB ring.[56]

Nucleotides Modulate Differently the Stability and Hydrodynamic Properties of the ClpB Hexamer. The effect of ADP and ATP on the self-association properties of ClpB was studied by composition-gradient light scattering and compared with the association behavior of the nucleotide-free (apo) protein. In contrast to other equilibrium methods, this novel technique allowed the fast (order of minutes) quantitative characterization of the oligomerization state of ClpB in the presence of ATP under conditions where less than 3% of the initially added nucleotide was hydrolyzed. Thus, it provides accurate values of molecular weights, complex stoichiometries, and association

Table 3. Effect of Nucleotides on the Self-Association of wt ClpB and $ClpB_{\Delta(410-455)}$ at 150 mM KCl As Determined by CG-SLS Measurements[a]

protein	log K'_6[b]	ΔG°_6[c] (kJ/mol)
apo-wt	12.8 ± 1.0 (13.0)[d]	−74 (−75)[d]
ADP-wt	16.2 ± 1.5	−94
ATP-wt	18.0 ± 2.0	−104
apo-$ClpB_{\Delta(410-455)}$	9.3 ± 1.0 (8.8)[d]	−53 (−51.0)[d]
ADP-$ClpB_{\Delta(410-455)}$	13.5 ± 2.0	−78
ATP-$ClpB_{\Delta(410-455)}$	14.9 ± 0.5	−86

[a] Model 8 was used to calculate the self-association parameters. [b] Association constants are expressed in molar units. [c] The standard-state free energy change was calculated from the relation $\Delta G^\circ_n = -2.3RT \log K_n$. [d] The values in parentheses correspond to best-fit parameters obtained from sedimentation equilibrium.

constants for ClpB in its ATP-bound state. Experiments were conducted under the same conditions used above to characterize apoClpB self-association (150 mM KCl), and a protein monomer concentration of <10 μM to decrease the relative abundance of large oligomers that would contribute much more to the experimental scattering.

The dependence of the weight-average molecular weight (calculated from R/K_{opt} using eq 1) on protein concentration is shown in Figure 5A for apo and nucleotide-bound wt ClpB. Data were quantitatively fitted with model 8, which also accounted for the sedimentation equilibrium data (see above), and the best fit calculated using the values listed in Table 3 is also shown in Figure 5A for each protein state (solid lines). It should be noted that none of the models that neglected the dodecameric species properly fitted the experimental data. The good agreement between the CG-SLS and sedimentation equilibrium results for apoClpB (also shown in Figure 5A) supported the robustness of this experimental approach. The values of both R/K_{opt} and M_W as a function of protein concentration were significantly higher for nucleotide-bound ClpB than for apoClpB, the effect being more pronounced for ATP-ClpB at low protein concentrations. This was reflected in the observed nucleotide-induced increase in the values of log K_6 (Table 3), and the mass fraction of the more abundant species (monomer and hexamer) estimated according to association scheme 8 (Figure S6 of the Supporting Information). The same experimental approach was used to characterize how nucleotides affected the self-association properties of M domain deletion mutant $ClpB_{\Delta(410-455)}$ (Figure 5B). As seen from the dependence of M_W on the protein concentration of apo and nucleotide-bound $ClpB_{\Delta(410-455)}$ (symbols) and from the K_6 values derived from model 8

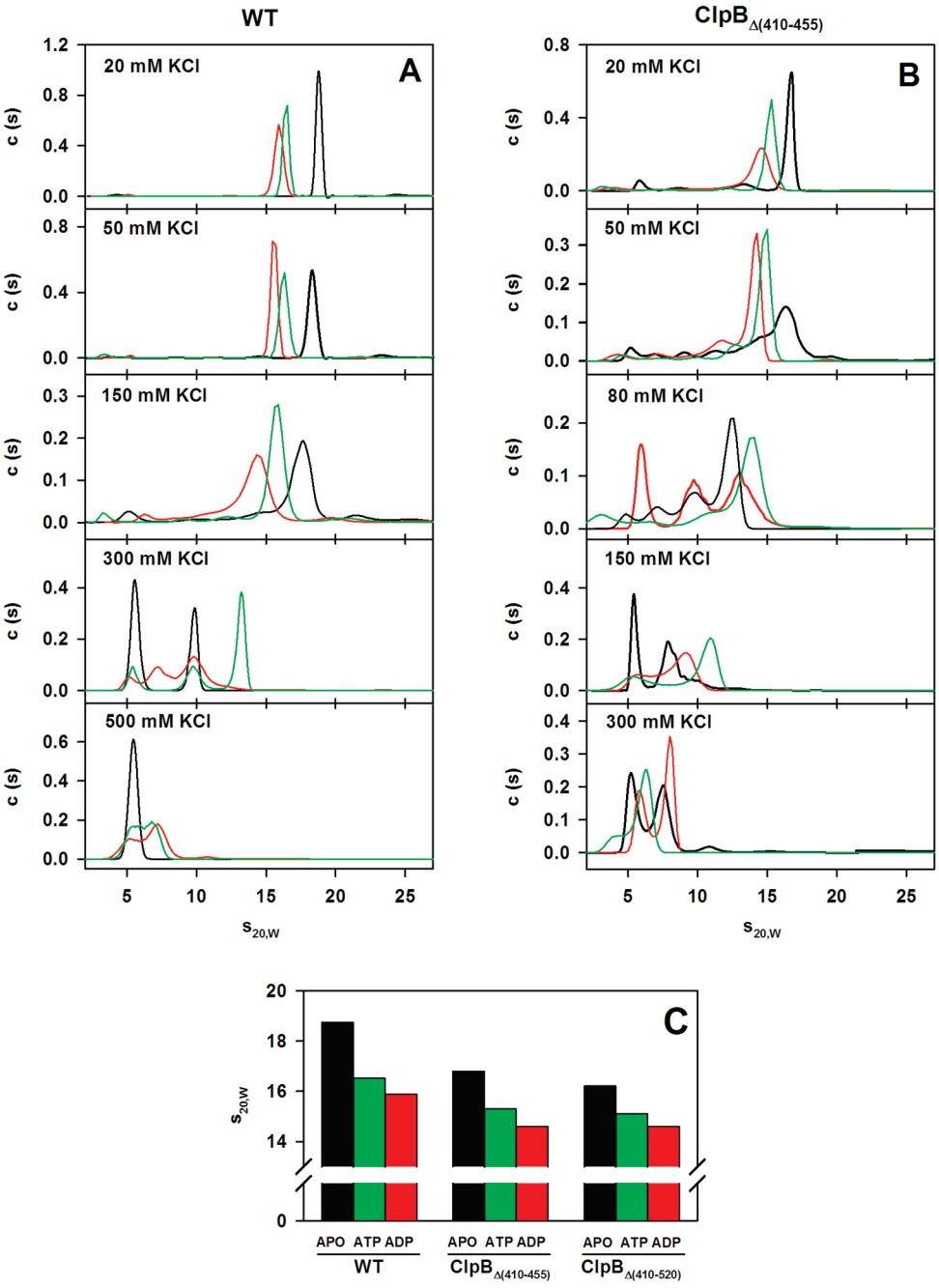

Figure 6. Effect of nucleotides on the hydrodynamic properties of wt ClpB and M domain deletion mutants. (A) Sedimentation coefficient distribution of wt ClpB (10 μM monomer) in the absence (black lines) and presence of 1 ADP (red lines) or ATP (green lines), at increasing KCl concentrations. In the presence of ATP, the sample also contains an ATP-regenerating system, as stated in Materials and Methods. (B) Same as panel A but for $ClpB_{\Delta(410-455)}$. (C) $s_{20,w}$ values of wt ClpB and ClpB M domain deletion mutants obtained as described for panel A in buffer contining 20 mM KCl.

(Table 3), a similar nucleotide-induced stabilization of the protein hexamer was observed for this deletion mutant. The apo form of both proteins was stabilized by ADP and ATP binding 30−33 and 20−25 kJ/mol, respectively, suggesting that nucleotide-induced stabilization of the protein hexamer involves structural elements different from the M domain. A similar effect was observed for $ClpB_{\Delta(410-520)}$ (not shown). These results also demonstrate that ADP- and ATP-bound ClpB hexamers are energetically different and therefore suggest that cycling between these conformations might help oligomer rearrangement during the functional cycle of the protein.

The effect of ADP and ATP on the sedimentation coefficient distribution of wt ClpB and both deletion mutants (10 μM monomer) is illustrated in Figure 6. An enzymatic nucleotide regeneration system maintained a steady-state ATP concentration during the experiment, as described in Materials and Methods. The salt dependence of the sedimentation profiles of wt ClpB (Figure 6A) and $ClpB_{\Delta(410-455)}$ (Figure 6B) indicated, as previously reported,[22,31,32] that nucleotides and especially ATP stabilized the protein oligomer under salt conditions that induced dissociation of their apo forms. The sensitivity of the liganded states to KCl concentration will be used to relate the

dx.doi.org/10.1021/bi101670s |*Biochemistry* 2011, 50, 1991–2003

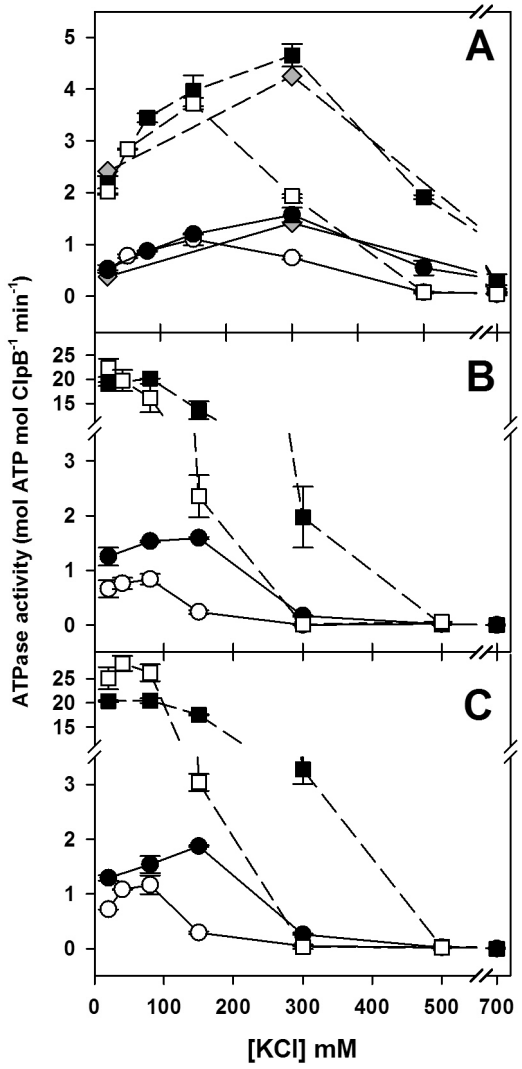

Figure 7. Effect of KCl on the ATPase activity of ClpB. (A) Steady-state ATPase activity of 2 μM (empty symbols) or 10 μM wt ClpB (filled symbols) in the absence (circles) and presence of α-casein (squares). Experiments were conducted at 25 °C and increasing KCl concentrations. The effect of NaCl on the activity of 2 μM ClpB is also shown (diamonds). (B and C) Same as panel A but for $ClpB_{\Delta(410-455)}$ and $ClpB_{\Delta(410-520)}$, respectively.

association and functional properties of the proteins (see below). Experiments performed at 20 mM KCl allow comparison of the sedimentation profiles of these proteins, because these experimental conditions favor oligomerization of the three nucleotide-free proteins. Apo-ClpB sedimented mainly with an $s_{20,w}$ value of ~18.5 S. This value was significantly lower in the presence of ADP (15.6 S) and ATP (16.3 S), most likely because of the known nucleotide-induced rearrangement of the oligomer structure.[21] The difference between the $s_{20,w}$ values of the ADP and ATP states of wt ClpB became larger with increasing salt concentrations up to 150 mM KCl (Figure S7 of the Supporting Information). If we assume that the nucleotide-induced expansion of the protein particle causes a decrease of the sedimentation coefficient, our data would indicate that this conformational change is greater in the ADP state than in the ATP state, in contrast to what can be theoretically estimated with HYDROMIC[57] for the same nucleotide-bound conformations of $ClpB_{Th}$: 19.7, 19.2, and 18.2 S for the apo, ADP, and ATP states, respectively.[21] This predictive method calculates the hydrodynamic properties of macromolecular complexes whose volumes are generated from electron microscopy images.[57]

Comparison of the $s_{20,w}$ values of wt ClpB and the deletion mutants at 20 mM KCl (Figure 6B) revealed that (i) deletion of motif 1 of the coiled coil had an effect similar to that of truncation of the whole M domain and (ii) the ADP-bound state of wt ClpB and both deletion mutants had the lowest sedimentation coefficient value. Deletion of the M domain reduced, but did not abolish, the difference between the $s_{20,w}$ values of the apo and nucleotide-bound conformations, supporting the possibility that although the coiled coil is involved in the nucleotide-induced conformational change, as previously reported,[20,21] structural regions other than the M domain also participate in this conformational transition. The difficulties mentioned above related to the effect that association kinetics might have on the complexity of sedimentation velocity boundaries preclude a more rigorous hydrodynamic analysis of these results.

Linking the Association and Functional Properties of ClpB. Our next goal was to establish a relationship between the association state and the ATPase and chaperone activities of these proteins under the same conditions employed in the SV experiments (10 μM ClpB). The ATPase activity of wt ClpB increased with KCl (or NaCl) concentration up to 300 mM, gradually decreased at higher salt concentrations, and was almost completely abolished at 700 mM KCl, in the absence and presence of α-casein (Figure 7A). The bell-shaped effect of salt on the ATPase activity of the protein differs from that described for Hsp104,[58] whose ATPase activity decreased with increasing NaCl concentrations. It has also been reported that the ATPase activity of $ClpB_{Eco}$[29] and the disaggregase activity of $ClpB_{Th}$[30] were inhibited, especially above 100 mM salt. This apparent discrepancy could be due to a lower stability of Hsp104 oligomer, which starts to dissociate above 20 mM NaCl.[59] The reason why the biphasic behavior observed here was not detected might be the source of the protein, in the case of $ClpB_{Th}$,[30] and/or the sensitivity of the method used to estimate the ATPase activity.[29] It should be mentioned that the enzymes used in the coupled assay (see Materials and Methods) were active at the highest KCl concentration assayed (not shown).

A similar salt dependence was obtained for the ATPase activity of $ClpB_{\Delta(410-455)}$ (Figure 7B) and $ClpB_{\Delta(410-520)}$ (Figure 7B). However, compared with the wt protein, the deletion mutants showed two differences. The first is the fact that the substrate-induced activation factor was 5−8 times larger than that of wt ClpB. This difference suggests that residues 410−455 of the M domain are involved in the substrate-induced conformational change that leads to ATPase activation. This finding indicates that the M domain, being in contact with the NBDs,[24,26] modulates their activity and controls the timing of the ATPase cycle in the presence of substrate proteins, in agreement with the proposed role of this domain in coupling the ATPase activity of both NBDs.[19,26,60,61] The second difference is that the highest ATPase activity of the mutants occurred at lower salt concentrations (150 mM KCl) and was almost completely inhibited at 500 mM KCl. This might be a consequence of the lower stability of their hexameric forms (see Table 2). If this were the case, lowering the ClpB concentration would favor dissociation of the protein hexamer under the same experimental conditions and should shift the ATPase activity curves toward lower KCl concentrations, as it is experimentally observed when the concentration of

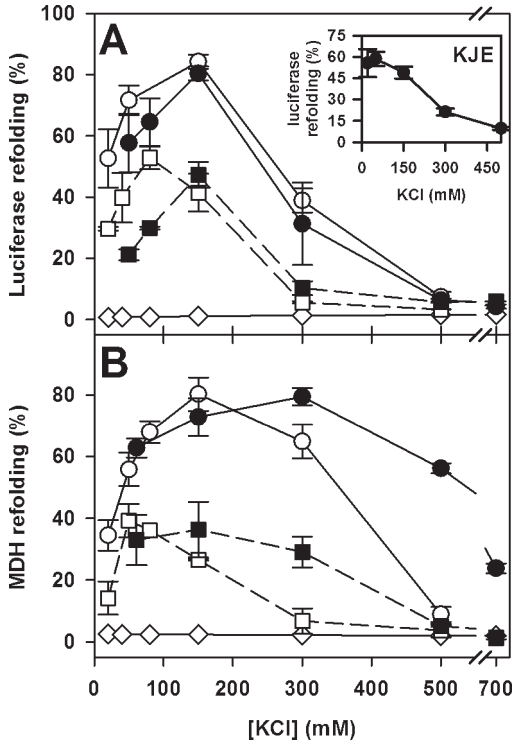

Figure 8. Sensitivity of the chaperone activity of ClpB to salt concentration. (A) Salt dependence of the reactivation of aggregated luciferase by the K system and 1.5 μM (empty symbols) or 10 μM (filled symbols) wt ClpB (circles) or $ClpB_{\Delta(410-455)}$ (squares). The inset shows the refolding of luciferase unfolded with Gdn-HCl by the K/J/E system alone. Substrate reactivation in the absence of chaperones (diamonds). (B) Reactivation of aggregated MDH by wt ClpB or $ClpB_{\Delta(410-455)}$ as a function of KCl concentration. Same symbols as in panel A.

the three proteins is reduced from 10 to 2 μM (Figure 7, empty symbols). Therefore, conditions that favor oligomerization also enhance the ATPase activity of the protein.

We next studied the salt dependence of the reactivation of luciferase (Figure 8A) and MDH (Figure 8B) aggregates by wt ClpB and the M domain deletion mutants. Remarkably, $ClpB_{\Delta(410-455)}$ was able to significantly reactivate these aggregates, in contrast to $ClpB_{\Delta(410-520)}$. Our data agree with the previously published finding that the M domain, and as seen here motif 2 of this domain, is essential for the display of a significant disaggregase activity. Luciferase reactivation by both proteins showed a salt dependence similar to that of the ATPase activity at 2 μM protein; however, the shift toward higher KCl concentrations at 10 μM protein described above was detected only for $ClpB_{\Delta(410-455)}$ (Figure 8A). To test whether this different behavior was due to a reduced activity of the K/J/E system and/or to a restricted ability of luciferase to refold at high ionic strengths, we measured the reactivation of luciferase unfolded in Gdn-HCl by the K system alone (Figure 8A, inset). Above 150 mM KCl, reactivation of luciferase by K/J/E is severely inhibited, and therefore, the use of this substrate might not allow distinguishing differences in chaperone activity at high salt concentrations. To avoid this limitation, we use MDH as an alternative substrate (Figure 8B). Chaperone-mediated reactivation of aggregated MDH followed the same salt dependence exhibited by the ATPase activity of both wt ClpB and $ClpB_{\Delta(410-520)}$. Increasing the ClpB concentration also induced a similar shift of the refolding curves toward higher salt concentrations. Thus, the same conditions were optimal for ATP hydrolysis and aggregate reactivation, as recently found for $ClpB_{Th}$.[62] Nevertheless, because of the complexity of the sample that contains chaperones and aggregated protein, we cannot rule out the possibility that interactions between these components could exert additional effects on the oligomerization state of ClpB and thus on its functional properties. The activation observed at low salt concentrations might be caused by a loosening of the subunit packing within the hexamer that could favor the conformational rearrangement associated with the functional cycle of the protein. A similar activation has been reported for heterohexamers composed of equimolar amounts of wt ClpB and a truncated form of the protein that lacks the N-terminal domain. The higher efficiency of the heterohexamer, as compared with that of wt ClpB, in protein aggregate reactivation was related to a favored nucleotide-induced conformational transition of the N-terminal domain whose mobility in the hybrid hexamer was not as restricted as in the full-length homohexamer.[63] A similar argument might apply in our case, because optimal functionality of wt ClpB is observed not under conditions of maximal stability of the hexamer ($\Delta G_6 = -121$ kJ/mol at 50 mM mM KCl) but when the hexamer is destabilized due to a moderate increase in salt concentration ($\Delta G_6 = -58$ kJ/mol at 300 mM KCl). A further increase in the ionic strength of the medium (above 300 mM KCl at 10 μM ClpB) induces oligomer dissociation and the inhibition of both protein activities. The comparison of the ATPase activity, the chaperone activity, and the association state of the protein suggests that the hexamer is most likely the active species *in vitro*, as postulated for $ClpB_{Th}$.[30]

CONCLUDING REMARKS

The main findings of this work indicate that the interplay among protein, salt concentration, and ligand binding modulates the oligomerization state of ClpB, which in turn controls its functional state. They show that the M domain is engaged in intersubunit interactions that stabilize the oligomeric structure of the protein and couples the ATPase activity of both NBDs, especially in the presence of substrate proteins. Finally, they also quantitatively demonstrate that the association free energy of the hexameric forms of wt ClpB and the M domain deletion mutants depends on the nature of the bound nucleotide, because $\Delta G_{(ATP-ADP)}$ is -10 and -8 kJ/mol for wt ClpB and $ClpB_{\Delta(410-520)}$, respectively. This difference in stability might be related to the role of oligomer assembly and disassembly in the functional cycle of the protein.[28,64] Nucleotide exchange could facilitate the rearrangement of the protein particle that aids ClpB to handle different client proteins or energetic events that might occur during protein disaggregation.[28]

ASSOCIATED CONTENT

Supporting Information. A detailed study of the effect of salt and nucleotides on the association equilibrium of wt ClpB and both M domain deletion mutants. This material is available free of charge via the Internet at http://pubs.acs.org.

AUTHOR INFORMATION

Corresponding Author

*G.R.: e-mail, grivas@cib.csic.es; phone, +34918373112; fax, +34915360432. A. Muga: e-mail, arturo.muga@ehu.es; phone, +34946012624; fax, +34946013500.

Present Addresses

[§]Division of Molecular Embryology, German Cancer Research Center, Im Neuenheimer Feld 581, Heidelberg 69120, Germany.

Funding Sources

This work was supported by the Ministerio de Educación y Ciencia (Grants BFU2007-64452 and BIO2008-04478-C03-03 to A. Muga and G.R., respectively), the Universidad del País Vasco and Gobierno Vasco (Grant IT-358-07), and Diputación Foral de Bizkaia (Grant DIPE08/19). U.d.C. and A. Martos are recipients of fellowships from the Ministerio de Educación y Ciencia, and S.P.A. was a fellow of the Gobierno Vasco. F.M. is supported by a Ramón y Cajal contract.

■ ACKNOWLEDGMENT

We thank A. Ortega (Departamento de Química Física, Facultad de Química, Universidad de Murcia, Murcia, Spain) for running the HYDROMIC algorithm, R. Ahijado (CIB) for his help with CG-SLC experiments, E. Bilbao for technical assistance, A. Minton (National Institutes of Health) for kindly providing the MATLAB scripts for the analysis of the association equilibria and fruitful discussions, and B. Monterroso (CIB) for useful comments.

■ ABBREVIATIONS

M domain, middle domain; Hsp, heat shock protein; $ClpB_{\Delta(410-455)}$, ClpB mutant from which residues 410−455 had been deleted; $ClpB_{\Delta(410-520)}$, ClpB deletion mutant from which residues 410−520 had been deleted; $ClpB_{Eco}$, ClpB from *E. coli*; $ClpB_{Th}$, ClpB from *Thermus thermophilus*.

■ REFERENCES

(1) Beyer, A. (1997) Sequence analysis of the AAA protein family. *Protein Sci. 6*, 2043–2058.

(2) Neuwald, A. F., Aravind, L., Spouge, J. L., and Koonin, E. V. (1999) AAA^+: A class of chaperone-like ATPases associated with the assembly, operation, and disassembly of protein complexes. *Genome Res. 9*, 27–43.

(3) Ogura, T., and Wilkinson, A. J. (2001) AAA^+ superfamily ATPases: Common structure−diverse function. *Genes Cells 6*, 575–597.

(4) Maurizi, M. R., and Xia, D. (2004) Protein binding and disruption by Clp/Hsp100 chaperones. *Structure 12*, 175–183.

(5) Sauer, R. T., Bolon, D. N., Burton, B. M., Burton, R. E., Flynn, J. M., Grant, R. A., Hersch, G. L., Joshi, S. A., Kenniston, J. A., Levchenko, I., Neher, S. B., Oakes, E. S., Siddiqui, S. M., Wah, D. A., and Baker, T. A. (2004) Sculpting the proteome with AAA^+ proteases and disassembly machines. *Cell 119*, 9–18.

(6) Mogk, A., Haslberger, T., Tessarz, P., and Bukau, B. (2008) Common and specific mechanisms of AAA^+ proteins involved in protein quality control. *Biochem. Soc. Trans. 36*, 120–125.

(7) Parsell, D. A., Kowal, A. S., Singer, M. A., and Lindquist, S. (1994) Protein disaggregation mediated by heat-shock protein Hsp104. *Nature 372*, 475–478.

(8) Weibezahn, J., Schlieker, C., Tessarz, P., Mogk, A., and Bukau, B. (2005) Novel insights into the mechanism of chaperone-assisted protein disaggregation. *Biol. Chem. 386*, 739–744.

(9) Glover, J. R., and Lindquist, S. (1998) Hsp104, Hsp70, and Hsp40: A novel chaperone system that rescues previously aggregated proteins. *Cell 94*, 73–82.

(10) Goloubinoff, P., Mogk, A., Zvi, A. P., Tomoyasu, T., and Bukau, B. (1999) Sequential mechanism of solubilization and refolding of stable protein aggregates by a bichaperone network. *Proc. Natl. Acad. Sci. U.S.A. 96*, 13732–13737.

(11) Motohashi, K., Watanabe, Y., Yohda, M., and Yoshida, M. (1999) Heat-inactivated proteins are rescued by the DnaK.J-GrpE set and ClpB chaperones. *Proc. Natl. Acad. Sci. U.S.A. 96*, 7184–7189.

(12) Zolkiewski, M. (1999) ClpB cooperates with DnaK, DnaJ, and GrpE in suppressing protein aggregation. A novel multi-chaperone system from *Escherichia coli*. *J. Biol. Chem. 274*, 28083–28086.

(13) Sanchez, Y., and Lindquist, S. L. (1990) HSP104 required for induced thermotolerance. *Science 248*, 1112–1115.

(14) Squires, C. L., Pedersen, S., Ross, B. M., and Squires, C. (1991) ClpB is the *Escherichia coli* heat shock protein F84.1. *J. Bacteriol. 173*, 4254–4262.

(15) Schirmer, E. C., Glover, J. R., Singer, M. A., and Lindquist, S. (1996) HSP100/Clp proteins: A common mechanism explains diverse functions. *Trends Biochem. Sci. 21*, 289–296.

(16) Barnett, M. E., Nagy, M., Kedzierska, S., and Zolkiewski, M. (2005) The amino-terminal domain of ClpB supports binding to strongly aggregated proteins. *J. Biol. Chem. 280*, 34940–34945.

(17) Beinker, P., Schlee, S., Groemping, Y., Seidel, R., and Reinstein, J. (2002) The N terminus of ClpB from *Thermus thermophilus* is not essential for the chaperone activity. *J. Biol. Chem. 277*, 47160–47166.

(18) Barnett, M. E., Zolkiewska, A., and Zolkiewski, M. (2000) Structure and activity of ClpB from *Escherichia coli*. Role of the amino- and carboxyl-terminal domains. *J. Biol. Chem. 275*, 37565–37571.

(19) Cashikar, A. G., Schirmer, E. C., Hattendorf, D. A., Glover, J. R., Ramakrishnan, M. S., Ware, D. M., and Lindquist, S. L. (2002) Defining a pathway of communication from the C-terminal peptide binding domain to the N-terminal ATPase domain in a AAA protein. *Mol. Cell 9*, 751–760.

(20) Lee, S., Sowa, M. E., Watanabe, Y. H., Sigler, P. B., Chiu, W., Yoshida, M., and Tsai, F. T. (2003) The structure of ClpB: A molecular chaperone that rescues proteins from an aggregated state. *Cell 115*, 229–240.

(21) Lee, S., Choi, J. M., and Tsai, F. T. (2007) Visualizing the ATPase cycle in a protein disaggregating machine: Structural basis for substrate binding by ClpB. *Mol. Cell 25*, 261–271.

(22) Mogk, A., Schlieker, C., Strub, C., Rist, W., Weibezahn, J., and Bukau, B. (2003) Roles of individual domains and conserved motifs of the AAA^+ chaperone ClpB in oligomerization, ATP hydrolysis, and chaperone activity. *J. Biol. Chem. 278*, 17615–17624.

(23) Kedzierska, S., Akoev, V., Barnett, M. E., and Zolkiewski, M. (2003) Structure and function of the middle domain of ClpB from *Escherichia coli*. *Biochemistry 42*, 14242–14248.

(24) Schirmer, E. C., Homann, O. R., Kowal, A. S., and Lindquist, S. (2004) Dominant gain-of-function mutations in Hsp104p reveal crucial roles for the middle region. *Mol. Biol. Cell 15*, 2061–2072.

(25) Lee, U., Wie, C., Escobar, M., Williams, B., Hong, S. W., and Vierling, E. (2005) Genetic analysis reveals domain interactions of *Arabidopsis* Hsp100/ClpB and cooperation with the small heat shock protein chaperone system. *Plant Cell 17*, 559–571.

(26) Haslberger, T., Weibezahn, J., Zahn, R., Lee, S., Tsai, F. T., Bukau, B., and Mogk, A. (2007) M domains couple the ClpB threading motor with the DnaK chaperone activity. *Mol. Cell 25*, 247–260.

(27) Weibezahn, J., Schlieker, C., Bukau, B., and Mogk, A. (2003) Characterization of a trap mutant of the AAA^+ chaperone ClpB. *J. Biol. Chem. 278*, 32608–32617.

(28) Werbeck, N. D., Schlee, S., and Reinstein, J. (2008) Coupling and dynamics of subunits in the hexameric AAA^+ chaperone ClpB. *J. Mol. Biol. 378*, 178–190.

(29) Kim, K. I., Cheong, G. W., Park, S. C., Ha, J. S., Woo, K. M., Choi, S. J., and Chung, C. H. (2000) Heptameric ring structure of the heat-shock protein ClpB, a protein-activated ATPase in *Escherichia coli*. *J. Mol. Biol. 303*, 655–666.

(30) Schlee, S., Groemping, Y., Herde, P., Seidel, R., and Reinstein, J. (2001) The chaperone function of ClpB from *Thermus thermophilus* depends on allosteric interactions of its two ATP-binding sites. *J. Mol. Biol. 306*, 889–899.

(31) Akoev, V., Gogol, E. P., Barnett, M. E., and Zolkiewski, M. (2004) Nucleotide-induced switch in oligomerization of the AAA^+ ATPase ClpB. *Protein Sci. 13*, 567–574.

(32) Zolkiewski, M., Kessel, M., Ginsburg, A., and Maurizi, M. R. (1999) Nucleotide-dependent oligomerization of ClpB from *Escherichia coli*. *Protein Sci. 8*, 1899–1903.

(33) Woo, K. M., Kim, K. I., Goldberg, A. L., Ha, D. B., and Chung, C. H. (1992) The heat-shock protein ClpB in *Escherichia coli* is a protein-activated ATPase. *J. Biol. Chem. 267*, 20429–20434.

(34) Moro, F., Fernandez, V., and Muga, A. (2003) Interdomain interaction through helices A and B of DnaK peptide binding domain. *FEBS Lett. 533*, 119–123.

(35) Zylicz, M., Yamamoto, T., McKittrick, N., Sell, S., and Georgopoulos, C. (1985) Purification and properties of the dnaJ replication protein of *Escherichia coli*. *J. Biol. Chem. 260*, 7591–7598.

(36) Mehl, A. F., Heskett, L. D., and Neal, K. M. (2001) A GrpE mutant containing the NH_2-terminal "tail" region is able to displace bound polypeptide substrate from DnaK. *Biochem. Biophys. Res. Commun. 282*, 562–569.

(37) Pace, C. N. (1986) Determination and analysis of urea and guanidine hydrochloride denaturation curves. *Methods Enzymol. 131*, 266–280.

(38) Norby, J. G. (1988) Coupled assay of Na^+,K^+-ATPase activity. *Methods Enzymol. 156*, 116–119.

(39) Schlieker, C., Tews, I., Bukau, B., and Mogk, A. (2004) Solubilization of aggregated proteins by ClpB/DnaK relies on the continuous extraction of unfolded polypeptides. *FEBS Lett. 578*, 351–356.

(40) Schuck, P. (2000) Size-distribution analysis of macromolecules by sedimentation velocity ultracentrifugation and lamm equation modeling. *Biophys. J. 78*, 1606–1619.

(41) Schuck, P., Perugini, M. A., Gonzales, N. R., Howlett, G. J., and Schubert, D. (2002) Size-distribution analysis of proteins by analytical ultracentrifugation: Strategies and application to model systems. *Biophys. J. 82*, 1096–1111.

(42) Holde, K. E. v. (1985) Sedimentation. In *Physical biochemistry*, 2nd ed., pp 110−136, Prentice-Hall, Englewood Cliffs, NJ.

(43) Laue, T. M., Shah, B. D., Ridgeway, T. M., and Pelletier, S. L. (1992) Computer-aided interpretation of analytical sedimentation data for proteins. In *Analytical Ultracentrifugation in Biochemistry and Polymer Science* (Harding, S. E., Rowe, A. J., and Horton, J., Eds.) pp 90−125, Royal Society of Chemistry, Cambridge, U.K.

(44) Minton, A. P. (1996) in *Modern Analytical Ultracentrifugation* (Schuster, T. M., and Laue, T. M., Eds.) pp 81−93, Birkhauser, Boston.

(45) Attri, A. K., and Minton, A. P. (2005) New methods for measuring macromolecular interactions in solution via static light scattering: Basic methodology and application to nonassociating and self-associating proteins. *Anal. Biochem. 337*, 103–110.

(46) Stacey, K. A. (1956) in *Light scattering in physical chemistry*, Chapter 2, Academic Press, New York.

(47) Saroff, H. A. (1989) Evaluation of uncertainties for parameters in binding studies: The sum-of-squares profile and Monte Carlo estimation. *Anal. Biochem. 176*, 161–169.

(48) Diamant, S., Rosenthal, D., Azem, A., Eliahu, N., Ben-Zvi, A. P., and Goloubinoff, P. (2003) Dicarboxylic amino acids and glycine-betaine regulate chaperone-mediated protein-disaggregation under stress. *Mol. Microbiol. 49*, 401–410.

(49) Haslberger, T., Zdanowicz, A., Brand, I., Kirstein, J., Turgay, K., Mogk, A., and Bukau, B. (2008) Protein disaggregation by the AAA^+ chaperone ClpB involves partial threading of looped polypeptide segments. *Nat. Struct. Mol. Biol. 15*, 641–650.

(50) Wendler, P., Shorter, J., Plisson, C., Cashikar, A. G., Lindquist, S., and Saibil, H. R. (2007) Atypical AAA^+ subunit packing creates an expanded cavity for disaggregation by the protein-remodeling factor Hsp104. *Cell 131*, 1366–1377.

(51) Werbeck, N. D., Kellner, J. N., Barends, T. R., and Reinstein, J. (2009) Nucleotide binding and allosteric modulation of the second AAA^+ domain of ClpB probed by transient kinetic studies. *Biochemistry 48*, 7240–7250.

(52) Mogk, A., Tomoyasu, T., Goloubinoff, P., Rudiger, S., Roder, D., Langen, H., and Bukau, B. (1999) Identification of thermolabile *Escherichia coli* proteins: Prevention and reversion of aggregation by DnaK and ClpB. *EMBO J. 18*, 6934–6949.

(53) Record, M. T., Jr., Courtenay, E. S., Cayley, D. S., and Guttman, H. J. (1998) Responses of *E. coli* to osmotic stress: Large changes in amounts of cytoplasmic solutes and water. *Trends Biochem. Sci. 23*, 143–148.

(54) Howlett, G. J., Minton, A. P., and Rivas, G. (2006) Analytical ultracentrifugation for the study of protein association and assembly. *Curr. Opin. Chem. Biol. 10*, 430–436.

(55) Abril, A. M., Salas, M., Andreu, J. M., Hermoso, J. M., and Rivas, G. (1997) Phage ϕ29 protein p6 is in a monomer-dimer equilibrium that shifts to higher association states at the millimolar concentrations found in vivo. *Biochemistry 36*, 11901–11908.

(56) Nagy, M., Akoev, V., and Zolkiewski, M. (2006) Domain stability in the AAA^+ ATPase ClpB from *Escherichia coli*. *Arch. Biochem. Biophys. 453*, 63–69.

(57) Garcia de la Torre, J., Llorca, O., Carrascosa, J. L., and Valpuesta, J. M. (2001) HYDROMIC: Prediction of hydrodynamic properties of rigid macromolecular structures obtained from electron microscopy images. *Eur. Biophys. J. 30*, 457–462.

(58) Schirmer, E. C., Queitsch, C., Kowal, A. S., Parsell, D. A., and Lindquist, S. (1998) The ATPase activity of Hsp104, effects of environmental conditions and mutations. *J. Biol. Chem. 273*, 15546–15552.

(59) Hattendorf, D. A., and Lindquist, S. L. (2002) Cooperative kinetics of both Hsp104 ATPase domains and interdomain communication revealed by AAA sensor-1 mutants. *EMBO J. 21*, 12–21.

(60) Watanabe, Y. H., Nakazaki, Y., Suno, R., and Yoshida, M. (2009) Stability of the two wings of the coiled-coil domain of ClpB chaperone is critical for its disaggregation activity. *Biochem. J. 421*, 71–77.

(61) Sielaff, B., and Tsai, F. T. (2010) The M-domain controls Hsp104 protein remodeling activity in an Hsp70/Hsp40-dependent manner. *J. Mol. Biol. 402*, 30–37.

(62) Hoskins, J. R., Doyle, S. M., and Wickner, S. (2009) Coupling ATP utilization to protein remodeling by ClpB, a hexameric AAA^+ protein. *Proc. Natl. Acad. Sci. U.S.A. 106*, 22233–22238.

(63) Nagy, M., Guenther, I., Akoyev, V., Barnett, M. E., Zavodszky, M. I., Kedzierska-Mieszkowska, S., and Zolkiewski, M. (2010) Synergistic cooperation between two ClpB isoforms in aggregate reactivation. *J. Mol. Biol. 396*, 697–707.

(64) Barends, T. R., Werbeck, N. D., and Reinstein, J. (2010) Disaggregases in 4 dimensions. *Curr. Opin. Struct. Biol. 20*, 46–53.